Diamidonaphthalene-Stabilized N-Heterocyclic Pnictogenium Cations and Their Cation−Cation Solid-State Interactions

Heather A. Spinney,[†] Ilia Korobkov,[†] Gino A. DiLabio,[‡] Glen P. A. Yap,[§] and Darrin S. Richeson*,[†]

Center for Catalysis Research and Innovation, Department of Chemistry, University of Ottawa, Ottawa, Ontario, Canada K1N 6N5, National Institute for Nanotechnology, National Research Council of Canada, 11421 Saskatchewan Drive, Edmonton, Alberta, Canada T6G 2M9, and Department of Chemistry and Biochemistry, University of Delaware, Newark, Delaware 19716

Received May 4, 2007

The synthesis and comprehensive characterization of a new series of N-heterocyclic phosphine, arsine, and stibine compounds is presented. The diamidochloropnictines $ClPn(NR)_2C_{10}H_6$ (Pn = P, As, Sb) were prepared via the dehydrohalide coupling reactions of *N*,*N*′-diisopropyl-1,8-diaminonaphthalene, $(^iPrNH)_2C_{10}H_6$, or *N*,*N*′-diphenyl-1,8-diaminonaphthalene, $(PhNH)_2C_{10}H_6$, with the appropriate pnictogen trichloride. Reaction of these pnictines with appropriate halide abstraction agents yielded the corresponding phosphenium and arsenium salts. These planar pnictogenium cations $\{Pn(NR)_2C_{10}H_6\}^+$ (Pn = P, As; R = ^{i}Pr, Ph) display dicoordinate pnictogen centers that are stabilized by an electron-rich diamidonaphthalene framework and represent rare examples of six-membered N-heterocyclic pnictogenium cations possessing a π-conjugated carbon backbone. The related stibenium salts could not be prepared via this route; however, the reaction of the new heteroleptic triamidostibene, $(Me_2N)Sb(^iPrN)_2C_{10}H_6$, with triflic acid does generate the base-stabilized stibenium cation, $[Sb(^iPrN)_2C_{10}H_6{\cdot}(Me_2NH)]^+$. The phosphenium and arsenium salts exhibit different modes of packing in their solid-state structures depending upon the identity of the nitrogen substituents. The two phenyl substituted compounds display an interaction between the pnictogen center and the π-system of an adjacent naphthyl moiety. In contrast, the isopropyl substituted species undergo metastable dimerization through naphthyl π-stacking. These dimers are bound by strong dipole−dipole and dispersion interactions as revealed through computational studies.

Introduction

Pnictogenium cations are six-electron, dicoordinate group 15 species containing lone pairs of electrons and vacant p-orbitals and accordingly display amphoteric properties as Lewis acids and bases. The electron deficient, coordinatively unsaturated element centers characteristic of these compounds attract interest from a fundamental perspective and ultimately provide for their interesting reactivity and synthetic utility. Like the now ubiquitous N-heterocyclic carbenes (NHCs), and their heavier congeners (**1**), successful isolation of the isoelectronic pnictogenium cations relies on heteroatom bonding and charge delocalization through incorporation of the pnictogen atom into a conjugated π-electron system.[1,2] Following the discovery of the first stable phosphenium ion some 40 years ago,[3] the sustained interest in related group 15 compounds has led to the isolation of a number of N-heterocyclic phosphenium,[4−6] arsenium,[7−9] and stibenium[10−12] cations represented by **2**−**6**. While some varieties of molecular structures have been reported, these species are principally dominated by a cyclic five-membered 1,3,2-diazapnictogenium species (**2**).

This paper concerns the isolation and characterization of pnictogenium cations (**7**) supported by the N,N′-disubstituted 1,8-diamidonaphthalene (R_2DAN^{2-}) framework.[13−15] These molecules possess a novel topology and electronic framework in which the dicoordinate pnictogen center resides in a π-electron-rich, six-membered heterocyclic ring. The geometric and electronic features of the R_2DAN^{2-} ligand are reminiscent

* Corresponding author. E-mail: darrin@uottawa.ca.
† University of Ottawa.
‡ National Research Council of Canada.
§ University of Delaware.

(1) For selected recent examples, see: (a) Hill, N. J.; West, R. *J. Organomet. Chem.* **2004**, *689*, 4165. (b) Kuhl, O. *Coord. Chem. Rev.* **2004**, *248*, 411. (c) Fedushkin, I. L.; Skatova, A. A.; Chudakova, V. A.; Khvoinova, N. M.; Baurin, A. Y.; Deckert, S.; Hummert, M.; Schumann, H. *Organometallics* **2004**, *23*, 3714. (d) Jing, H.; Edulji, S. K.; Gibbs, J. M.; Stern, C. L.; Zhou, H.; Nguyen, S. T. *Inorg. Chem.* **2004**, *43*, 4315. (e) Hitchcock, P. B.; Hu, J.; Lappert, M. F.; Severn, J. R. *Dalton Trans.* **2004**, 4193. (f) Richards, A. F.; Brynda, M.; Power, P. P. *Organometallics* **2004**, *23*, 4009.

(2) Bourissou, D.; Guerret, O.; Gabbaï, F. P.; Bertrand, G. *Chem. Rev.* **2000**, *100*, 39.

(3) Dimroth, K.; Hoffmann, P. *Angew. Chem., Int. Ed. Engl.* **1964**, *3*, 384.

(4) Reviews: (a) Cowley, A. H.; Kemp, R. *Chem. Rev.* **1985**, *85*, 367. (b) Gudat, D. *Coord. Chem. Rev.* **1997**, *173*, 71.

(5) Carmalt, C. J.; Lomeli, V.; McBurnett, B. G.; Cowley, A. H. *Chem. Commun.* **1997**, 2095.

(6) Reeske, G.; Hoberg, C. R.; Hill, N. J.; Cowley, A. H. *J. Am. Chem. Soc.* **2006**, *128*, 2800.

(7) Burford, N.; Parks, T. M.; Royan, B. W.; Borecka, B.; Cameron, T. S.; Richardson, J. F.; Gabe, E. J.; Haynes, R. *J. Am. Chem. Soc.* **1992**, *114*, 8147.

(8) Burford, N.; Macdonald, C. L. B.; Parks, T. M.; Wu, G.; Borecka, B.; Kwiatkowski, W.; Cameron, T. S. *Can. J. Chem.* **1996**, *74*, 2209.

(9) Reeske, G.; Cowley, A. H. *Chem. Commun.* **2006**, 1784.

(10) Gudat, D.; Gans-Eichler, T.; Nieger, M. *Chem. Commun.* **2004**, 2434.

(11) (a) Burck, S.; Daniels, J.; Gans-Eichler, T.; Gudat, D.; Nättinen, K.; Nieger, M. *Z. Anorg. Allg. Chem.* **2005**, *631*, 1403. (b) Gans-Eichler, T.; Gudat, D.; Nieger, M. *Heteroatom. Chem.* **2005**, *16*, 327.

(12) (a) Veith, M.; Bertsch, B.; Huch, V. *Z. Anorg. Allg. Chem.* **1988**, *559*, 73. (b) Veith, M.; Bertsch, B. *Z. Anorg. Allg. Chem.* **1988**, *557*, 7.

(13) (a) Spinney, H. A.; Yap, G. P. A.; Korobkov, I.; DiLabio, G. A.; Richeson, D. S. *Organometallics* **2006**, *25*, 3541. (b) Spinney, H. A.; Korobkov, I.; Richeson, D. S. *Chem. Commun.* **2007**, 1647.

10.1021/om7004436 CCC: $37.00
Publication on Web 08/23/2007

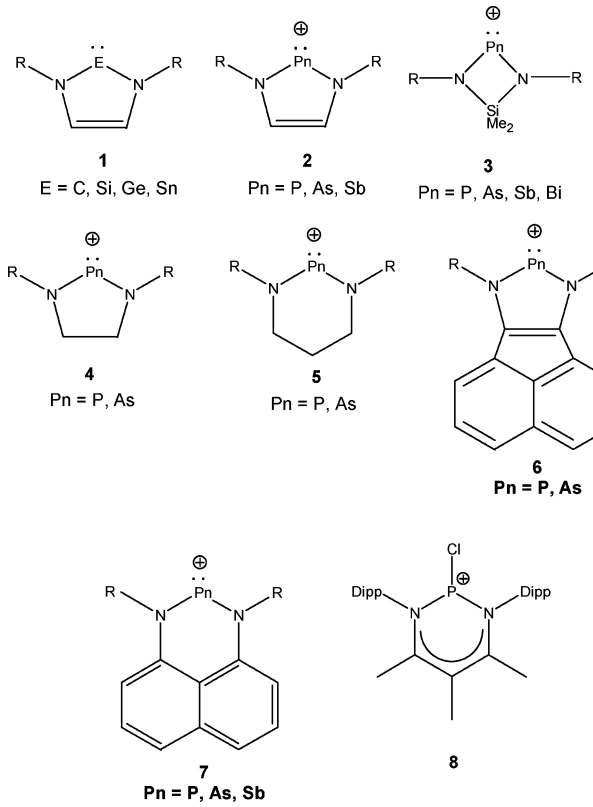

of the β-diketiminate scaffold;[16] however, among the significant differences between these two ligand arrays are the dianionic charge and naphthalene backbone of R_2DAN^{2-}. This latter feature prevents substitution reactions in the ligand backbone, and as such, we anticipated that R_2DAN^{2-} would be a more robust ligand than β-diketiminate. Interestingly, it is only recently that the first β-diketiminate supported phosphorus compound (**8**), an N,N′-chelated phosphenium cation, was isolated,[17] and computational studies suggest that β-diketiminate supported pnictogenium cations are inherently unstable.[18] The utilization of the R_2DAN^{2-} support structure for group 15 compounds promises to yield novel species with applications in coordination chemistry and catalysis.

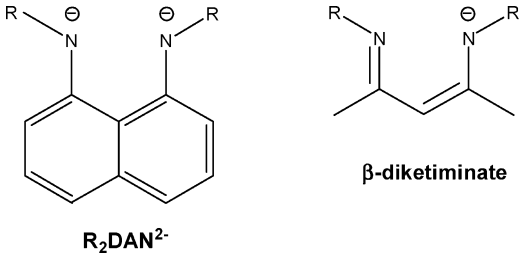

Experimental Procedures

General Methods. Reactions were performed using standard Schlenk techniques (N_2) or, alternatively, in a glove box with a nitrogen atmosphere. Triethylamine was dried by fractional distillation from KOH and then CaH_2. Dichloromethane was distilled over CaH_2 prior to use. All other solvents were sparged with nitrogen and then dried by passage through a column of activated alumina using an apparatus purchased from Anhydrous Engineering. Deuterated benzene and dichloromethane were dried using activated molecular sieves. Tris(dimethylamido)antimony was purchased from Strem Chemicals and used as received. All other chemicals were purchased from Aldrich and used without further purification. *N*,*N*′-Diisopropyl-1,8-diaminonaphthalene and *N*,*N*′-diphenyl-1,8-diaminonaphthalene were prepared according to previously reported procedures.[14a,19] NMR spectra were run on a Bruker Avance 300 MHz spectrometer with deuterated benzene or dichloromethane as a solvent and internal standard. Infrared spectra were collected on samples prepared as Nujol mulls on NaCl plates using a ABB Bomem MB Series FT-IR spectrometer and are reported in wavenumbers (cm^{-1}) followed by ranked intensities in parentheses, where a value of one corresponds to the most intense peak in the spectrum. Elemental analyses were performed by Guelph Chemical Laboratories, Guelph, ON, Canada, with the exception of elemental analyses of **10d** and **11b**, which were performed by Robertson Microlit Laboratories, Madison, NJ.

Computational Methods. Calculations were performed using the Gaussian 03 package of programs.[20] To obtain molecular orbitals for the pnictogenium cations, the positions of the hydrogen atoms on the crystal structures of the cations were optimized using the B971/6-31+G(d,p) functional. This functional was chosen because it can, to some extent, predict interactions in van der Waals complexes.[21] Additional calculations on π-stacked phosphenium cation dimers were performed using the MP2 approach with various basis sets.

X-ray. A suitable crystal was selected, mounted on a thin, glass fiber using viscous oil, and cooled to the data collection temperature. Data were collected on a Bruker AXS SMART 1k CCD diffractometer using 0.3° ω-scans at 0, 90, and 180° in φ. Initial unit cell parameters were determined from 60 data frames collected at different sections of the Ewald sphere. Semiempirical absorption corrections based on equivalent reflections were applied. The structures were solved by direct methods, completed with difference Fourier synthesis, and refined with full-matrix least-squares procedures based on F^2. All non-hydrogen atoms were refined with anisotropic displacement parameters. All hydrogen atoms were treated as idealized contributions. All scattering factors and anomalous dispersion factors are contained in the SHELXTL 6.12[37] program library. Relevant crystal data are reported in Tables 1 and 2, while selected bond distances and angles are reported in Table 3.

General Procedure for the Preparation of Diamidochloropnictines 9a−f. To a solution of 1,8-(^{i}PrNH)$_2$C$_{10}$H$_6$ (0.3−1 g) or 1,8-(PhNH)$_2$C$_{10}$H$_6$ (0.3−1 g) in 30 mL of toluene was added

(14) For applications of R_2DAN^{2-} to group 14, see: (a) Bazinet, P. Yap, G. P. A.; DiLabio, G. A.; Richeson, D. S. *Inorg. Chem.* **2005**, *44*, 4616. (b) Bazinet, P. Yap, G. P. A.; Richeson, D. S. *J. Am. Chem. Soc.* **2003**, *125*, 13314. (c) Bazinet, P.; Yap, G. P. A.; Richeson, D. S. *J. Am. Chem. Soc.* **2001**, *123*, 11162. (d) Ayers, A. G.; Drost, C. D.; Gehrhus, B.; Hitchcock, P. B.; Lappert, M. F. *Z. Anorg. Allg. Chem.* **2004**, *630*, 2090. (e) Drost, C.; Hitchcock, P. B.; Lappert, M. F. *Angew. Chem., Int. Ed.* **1999**, *38*, 1113. (f) Schaeffer, C. D., Jr.; Zuckerman, J. J. *J. Am. Chem. Soc.* **1974**, *96*, 7160.

(15) Further applications of R_2DAN^{2-} can be found in: (a) Lee, C. H.; La, Y.-H.; Park, J. W. *Organometallics* **2000**, *19*, 344. (b) Lee, C. H.; La, Y.-H.; Park, J.; Park, J. W. *Organometallics* **1998**, *17*, 3648. (c) Nomura, K.; Naga, N.; Takaoki, K. *Macromolecules* **1998**, *31*, 8009. (d) Galka, C. H.; Trösch, D. J. M.; Rüdenauer, I.; Gade, L. H.; Scowen, I. J.; McPartlin, M. *Inorg. Chem.* **2000**, *39*, 4615. (e) Hellmann, K. W.; Galka, C. H.; Rüdenauer, I.; Gade, L. H.; Scowen, I. J.; McPartlin, M. *Angew. Chem., Int. Ed.* **1998**, *37*, 1948. (f) Hellmann, K. W.; Galka, C. H.; Gade, L. H.; Steiner, A., Wright, D. S.; Kottke, T.; Stalke, D. *Chem. Commun.* **1998**, 549.

(16) For a recent review of β-diketiminates and their metal complexes, see: Bourget-Merle, L.; Lappert, M. F.; Severn, J. R. *Chem. Rev.* **2002**, *102*, 3031.

(17) Vidovic, D.; Lu, Z.; Reeske, G.; Moore, J. A.; Cowley, A. H. *Chem. Commun.* **2006**, 3501−3503.

(18) Ellis, B. D.; Macdonald, C. L. B. *Inorg. Chim. Acta* **2007**, *360*, 329.

(19) Bazinet, P.; Ong, T.-G.; O'Brien, J. S.; Lavoie, N.; Bell, E.; Yap, G. P. A.; Korobkov, I.; Richeson, D. S. *Organometallics* **2007**, *26*, 2885.

(20) Frisch, M. J.; et al. *Gaussian 03*, revision D.01; Gaussian, Inc.: Pittsburgh, PA, 2004.

(21) Johnson, E. R.; DiLabio, G. A. *Chem. Phys. Lett.* **2006**, *419*, 333−339.

Table 1. Crystal Data for Pnictines $ClPn(RN)_2C_{10}H_6$ (9a−c,e) and $(NMe_2)Sb(^iPrN)_2C_{10}H_6$ (14)

compound	**9a**[a]	**9b**	**9c**[b]	**9e**[b,c]	**14**[b]
formula	$C_{16}H_{20}N_2PCl$	$C_{22}H_{16}N_2PCl$	$C_{16}H_{20}N_2AsCl$	$C_{37.6}H_{46.4}N_4Sb_2Cl_2$	$C_{18}H_{26}N_3Sb$
molecular wt (g/mol)	306.76	374.79	350.71	868.79	406.17
cryst syst	monoclinic	monoclinic	monoclinic	monoclinic	orthorhombic
space group	$P2_1/n$	$C2/c$	$P2_1/n$	$P2_1/n$	$Pna2_1$
color	colorless	colorless	colorless	orange	yellow
a (Å)	8.796(2)	15.090(4)	8.8383(19)	15.669(4)	14.606(3)
b (Å)	16.226(4)	9.110(2)	16.434(3)	11.931(3)	9.7332(17)
c (Å)	11.612(3)	26.584(6)	11.551(2)	21.118(5)	12.573(2)
α (deg)	90	90	90	90	90
β (deg)	105.817(5)	92.548(4)	106.825(3)	92.125(4)	90
γ (deg)	90	90	90	90	90
V (Å^3)	1594.5(7)	3650.7(15)	1606.0(6)	3945.3(15)	1813.0(5)
Z	4	8	4	4	4
R^d ($I > 2\sigma(I)$)	0.0459	0.0492	0.0309	0.0456	0.0240
wR_2[e] (all data)	0.1179	0.1195	0.0763	0.1356	0.0643
GOF[f] (all data)	1.028	1.058	1.035	1.069	1.039
$\Delta\rho$ max and min (e Å^{-3})	+0.317, −0.177	+0.320, −0.213	+0.380, −0.247	+1.271, −0.596	+0.437, −0.394

[a] Previously reported (see ref 13a). [b] Previously reported (see ref 13b). [c] Unit cell contains two independent molecules of **9e** and 80% of a disordered toluene molecule. [d] $R_1 = (\Sigma|F_o^*| - |F_c|)/(\Sigma|F_o|)$. [e] $wR_2 = [(\Sigma w(F_o^2 - F_c^2)^2)/(\Sigma w(F_o^2)^2)]^{1/2}$. [f] GOF $= [(\Sigma w(F_o^2 - F_c^2)/(n - p)]^{1/2}$, where n = number of reflections and p = number of parameters.

Table 2. Crystal Data for Pnictogenium Cations $[Pn(RN)_2C_{10}H_6][GaCl_4]$ (10a−d), $[P(PhN)_2C_{10}H_6][OTf]$ (11b), and $[Sb(^iPrN)_2C_{10}H_6{\cdot}NHMe_2][OTf]$ (15)

compound	**10a**[a]	**10b**	**10c**[b,c]	**10d**	**11b**	**15**[b,d]
formula	$C_{16}H_{20}N_2PGaCl_4$	$C_{22}H_{16}N_2PGaCl_4$	$C_{17.75}H_{22}N_2AsGaCl_4$	$C_{22}H_{16}N_2AsGaCl_4$	$C_{23}H_{16}N_2O_3F_3PS$	$C_{38}H_{54}N_6O_6F_6Sb_2S_2$
molecular wt (g/mol)	482.83	550.86	549.81	594.81	488.41	1112.49
cryst syst	triclinic	monoclinic	monoclinic	monoclinic	monoclinic	triclinic
space group	$P\bar{1}$	$P2_1/c$	$P2_1/n$	$P2_1/c$	$P2_1/n$	$P\bar{1}$
color	red−orange	red	brown	red	orange	yellow
a (Å)	8.12(3)	10.133(3)	7.233(2)	10.106(3)	11.635(3)	8.5648(13)
b (Å)	11.36(4)	10.2962(16)	17.314(6)	10.307(3)	10.954(3)	9.7606(15)
c (Å)	11.99(4)	21.998(5)	19.580(7)	21.900(5)	17.175(4)	27.018(4)
α (deg)	64.86(5)	90	90	90	90	81.973(2)
β (deg)	89.70(6)	96.612(9)	99.501(6)	95.71(2)	91.358(3)	89.580(2)
γ (deg)	78.86(6)	90	90	90	90	81.727(2)
V (Å^3)	978(6)	2279.7(10)	2418.3(14)	2269.8(10)	2188.3(10)	2213.0(6)
Z	2	4	4	4	4	2
R^e ($I > 2\sigma(I)$)	0.0526	0.0335	0.0605	0.0428	0.0447	0.0379
wR_2[f] (all data)	0.1483	0.0905	0.1550	0.1146	0.1398	0.0963
GOF[g] (all data)	1.049	1.037	1.028	1.037	1.045	1.037
$\Delta\rho$ max and min (e Å^{-3})	+0.830, −0.452	+0.636, −0.247	+0.875, −0.439	+0.722, −0.697	+0.423, 0.253	+0.850, −0.472

[a] Previously reported (see ref 13a). [b] Previously reported (see ref 13b). [c] Unit cell contains 25% of a disordered toluene molecule. [d] Unit cell contains two independent units of **15**. [e] $R_1 = (\Sigma|F_o^*| - |F_c|)/(\Sigma|F_o|)$. [f] $wR_2 = [(\Sigma w(F_o^2 - F_c^2)^2)/(\Sigma w(F_o^2)^2)]^{1/2}$. [g] GOF $= [(\Sigma w(F_o^2 - F_c^2)/(n - p)]^{1/2}$, where n = number of reflections and p = number of parameters.

Table 3. Selected Bond Lengths (Å), Angles (deg), and ^{31}P NMR Chemical Shifts (ppm) for New Compounds 9a−c, 9e, 10a−d, 11b, 14, and 15

compound	Pn−X[a]	Pn−N(1)	Pn−N(2)	N(1)−C_{naph}	N(2)−C_{naph}	N−Pn−N	bend angle[b]	δ ^{31}P NMR
$ClP(^iPrN)_2C_{10}H_6$ (**9a**)	2.1723(9)	1.670(2)	1.670(2)	1.412(3)	1.409(3)	99.7(1)	31.7	102[c]
$ClP(PhN)_2C_{10}H_6$ (**9b**)	2.148(1)	1.678(2)	1.681(2)	1.422(3)	1.433(3)	98.9(1)	32.1	99[c]
$ClAs(^iPrN)_2C_{10}H_6$ (**9c**)	2.2820(8)	1.810(2)	1.812(2)	1.410(3)	1.413(3)	95.61(9)	31.9	
$ClSb(^iPrN)_2C_{10}H_6$[d] (**9e**)	2.392(2)	2.021(5)	2.017(4)	1.396(7)	1.394(7)	86.5(2)	39.6	
	2.4141(16)	2.014(4)	2.020(4)	1.411(7)	1.405(6)	87.98(18)	34.9	
$[P(^iPrN)_2C_{10}H_6][GaCl_4]$ (**10a**)	4.04(1)	1.609(8)	1.629(7)	1.410(9)	1.408(9)	105.4(3)	2.2	239[e]
$[P(PhN)_2C_{10}H_6][GaCl_4]$ (**10b**)	3.258(7)	1.633(2)	1.634(2)	1.435(2)	1.434(2)	103.17(8)	5.5	195[e]
$[As(^iPrN)_2C_{10}H_6][GaCl_4]$ (**10c**)	3.49(1)	1.762(7)	1.757(7)	1.437(11)	1.434(11)	101.4(3)	3.9	
$[As(PhN)_2C_{10}H_6][GaCl_4]$ (**10d**)	3.20(1)	1.771(3)	1.765(3)	1.424(4)	1.423(4)	98.8(1)	6.4	
$[P(PhN)_2C_{10}H_6][OTf]$ (**11b**)	2.594(5)	1.635(2)	1.632(2)	1.431(3)	1.430(3)	102.78(11)	4.0	120[c]
$(NMe_2)Sb(^iPrN)_2C_{10}H_6$ (**14**)	2.056(4)	2.022(3)	2.028(4)	1.382(5)	1.391(6)	86.2(2)	42.0	
$[Sb(^iPrN)_2C_{10}H_6{\cdot}NHMe_2][OTf]$[d] (**15**)	2.323(4)	1.997(4)	2.000(4)	1.424(6)	1.407(6)	93.0(2)	26.0	
	2.313(4)	1.988(4)	1.991(4)	1.410(6)	1.419(6)	92.77(17)	18.1	

[a] Pnictogen−halogen bond length or closest pnictogen−halogen contact. [b] Angle between naphthalene plane and N−Pn−N plane. [c] C_6D_6. [d] Two independent molecules in asymmetric unit. [e] CD_2Cl_2.

sequentially $PnCl_3$ (Pn = P or As: 1.3 equiv; Pn = Sb: 1 equiv) followed by NEt_3 (2.6 equiv). The reaction mixture was stirred for 4 days, during which time a copious amount of white precipitate formed, and the solution gradually turned colorless (P), yellow (As), or orange (Sb). All volatiles were removed under vacuum, toluene was added to the solid reaction mixture, and the solution was filtered through a glass frit packed with Celite. After removal of volatiles from the filtrate, the solid material obtained was recrystallized as outlined next.

$ClP(^iPrN)_2C_{10}H_6$ (9a). X-ray quality, colorless crystals of **9a** (0.265 g, 70%) were obtained by placing a concentrated hexane solution in the freezer at −20 °C overnight. ^{1}H NMR (C_6D_6): 1.2 (dd, $^3J_{HH}$ = 7 Hz, $^4J_{P-H}$ = 2 Hz, 6H, CH_3), 1.3 (dd, $^3J_{HH}$ = 7 Hz, $^4J_{P-H}$ = 0.5 Hz, 6H, CH_3), 3.8 (doublet of septets, $^3J_{P-H}$ = 18 Hz,

$^3J_{HH}$ = 7 Hz, 2H, C*H*Me$_2$), 6.6 (d, $^3J_{HH}$ = 8 Hz, 2H, *H*Ar), 7.2 (t, $^3J_{HH}$ = 8 Hz, 2H, *H*Ar), 7.3 (d, $^3J_{HH}$ = 8 Hz, 2H, *H*Ar). ^{13}C{^{1}H} NMR (C_6D_6): 21 (d, $^3J_{PC}$ = 15 Hz, *C*H$_3$), 24 (d, $^3J_{PC}$ = 21 Hz, *C*H$_3$), 51 (d, $^2J_{PC}$ = 28 Hz, *C*HMe$_2$), 109 (s, *C*HAr), 122 (s, *C*HAr), 127 (s, *C*HAr), 130 (s, *C*Ar), 137 (s, *C*Ar), 139 (d, $^2J_{PC}$ = 5 Hz, *C*Ar). ^{31}P{^{1}H} NMR (C_6D_6): 102 (s). IR: 1612(11), 1575(5), 1517-(16), 1324(13), 1301(12), 1249(16), 1192(15), 1178(12), 1168(11), 1141(8), 1087(8), 1050(9), 967(6), 943(11), 911(14), 895(14), 878-(10), 815(3), 800(3), 784(4), 761(2), 697(7), 635(1), 586(13), 551-(5). Anal. Calcd for $C_{16}H_{20}N_2PCl$: C 62.64, H 6.57, N 9.13; Found: C 62.37, H 6.30, N 9.24.

ClP(PhN)$_2$C$_{10}$H$_6$ (9b). X-ray quality, colorless crystals of **9b** (0.815 g, 67%) were obtained overnight by recrystallization from a 50:50 toluene/hexane mixture at −20 °C. ^{1}H NMR (C_6D_6): 6.5 (d, $^3J_{HH}$ = 8 Hz, 2H, *H*Ar), 6.9−7.1 (m, 8H, *H*Ar), 7.2 (d, $^3J_{HH}$ = 8 Hz, 2H, *H*Ar), 7.4 (d, $^3J_{HH}$ = 8 Hz, 4H, *H*Ar). ^{13}C{^{1}H} NMR (C_6D_6): 112 (s, *C*HAr), 119 (s, *C*Ar) 122 (s, *C*HAr), 127 (s, *C*HAr), 128.5 (d, $^4J_{PC}$ = 3 Hz, *C*HAr), 129.3 (d, $^3J_{PC}$ = 9 Hz, *C*HAr), 131 (s, *C*HAr), 136 (s, *C*Ar), 140 (d, $^2J_{PC}$ = 5 Hz, *C*Ar), 142 (d, $^2J_{PC}$ = 23 Hz, *C*Ar). ^{31}P{^{1}H} NMR (C_6D_6): 99 (s). IR: 1572(13), 1288-(14), 1275(14), 1209(15), 1159(15), 1055(14), 967(13), 907(12), 887(13), 860(10), 815(4), 786(5), 763(3), 756(3), 747(2), 727(3), 693(1), 634(8), 627(6), 615(10), 578(11), 540(7), 515(9). Anal. Calcd for $C_{22}H_{16}N_2PCl$: C 70.50, H 4.30, N 7.47; Found: C 70.43, H 4.65, N 7.36.

ClAs(*i*PrN)$_2$C$_{10}$H$_6$ (9c). X-ray quality, yellow crystals of **9c** (0.80 g, 55%) were obtained overnight by recrystallization from a 50:50 toluene/hexane mixture at −20 °C. ^{1}H NMR (C_6D_6): 1.1 (d, $^3J_{HH}$ = 7 Hz, 6H, C*H*$_3$), 1.3 (d, $^3J_{HH}$ = 6 Hz, 6H, C*H*$_3$), 3.9 (septet, $^3J_{HH}$ = 7 Hz, 2H, C*H*Me$_2$), 6.6 (d, $^3J_{HH}$ = 8 Hz, 2H, *H*Ar), 7.2 (t, $^3J_{HH}$ = 8 Hz, 2H, *H*Ar), 7.3 (dd, $^3J_{HH}$ = 8 Hz, $^4J_{HH}$ = 0.9 Hz, 2H, *H*Ar). ^{13}C{^{1}H} NMR (C_6D_6): 22 (s, *C*H$_3$), 25 (s, *C*H$_3$), 50 (s, *C*HMe$_2$), 108 (s, *C*HAr), 120.7 (s, *C*Ar), 121.4 (s, *C*HAr), 127 (s, *C*HAr), 138 (s, *C*Ar), 142 (s, *C*Ar). IR : 1923(13), 1821(18), 1740-(15), 1727(14), 1640(18), 1606(9), 1569(8), 1519(14), 1297(12), 1249(16), 1331(12), 1129(8), 1165(10), 1104(10), 1081(10), 1048-(7), 955(4), 878(6), 812(3), 870(4), 784(5), 762(1), 668(17), 632-(2), 565(11), 520(8). Anal. Calcd for $C_{16}H_{20}N_2AsCl$: C 54.79, H 5.75, N 7.99; Found: C 55.15, H 6.15, N 8.02.

ClAs(PhN)$_2$C$_{10}$H$_6$ (9d). Yellow, fibrous crystals of **9d** (0.712 g, 70%) were obtained overnight by recrystallization from a 50:50 toluene/hexane mixture at −20 °C. The crystals were not suitable for X-ray diffraction. ^{1}H NMR (CD_2Cl_2): 6.4 (d, $^3J_{HH}$ = 8 Hz, 2H, *H*Ar), 7.2 (t, $^3J_{HH}$ = 8 Hz, 2H, *H*Ar), 7.3 (d, $^3J_{HH}$ = 8 Hz, 2H, *H*Ar), 7.4−7.6 (m, 10H, *H*Ar). ^{13}C{^{1}H} NMR (CD_2Cl_2): 111 (s, *C*HAr), 119 (s, *C*Ar), 122 (s, *C*HAr), 127 (s, *C*HAr), 128.6 (s, *C*HAr), 129.0 (s, *C*HAr), 131 (s, *C*HAr), 137 (s, *C*Ar), 142 (s, *C*Ar), 143 (s, *C*Ar). IR : 1613(18), 1590(13), 1567(7), 1486(10), 1289-(12), 1273(14), 1256(15), 1210(14), 1165(11), 1073(18), 1047(9), 943(13), 932(7), 894(7), 862(18), 816(1), 808(6), 786(17), 759(5), 744(3), 727(4), 706(8), 697(2), 629(16), 622(10), 614(10). Anal. Calcd for $C_{22}H_{16}N_2AsCl$: C 63.10, H 3.85, N 6.69; Found: C 62.94, H 4.11, N 6.45.

ClSb(*i*PrN)$_2$C$_{10}$H$_6$ (9e). X-ray quality, orange crystals of **9e** (0.63 g, 38%) were obtained overnight by recrystallization from a 50:50 toluene/hexane mixture at −20 °C. ^{1}H NMR (C_6D_6): 1.1 (d, $^3J_{HH}$ = 6 Hz, 6H, C*H*$_3$), 1.2 (d, $^3J_{HH}$ = 6 Hz, 6H, C*H*$_3$), 4.1 (septet, $^3J_{HH}$ = 6 Hz, 2H, C*H*Me$_2$), 6.7 (d, $^3J_{HH}$ = 8 Hz, 2H, *H*Ar), 7.3 (t, $^3J_{HH}$ = 8 Hz, 2H, *H*Ar), 7.4 (d, $^3J_{HH}$ = 7 Hz, 2H, *H*Ar). ^{13}C{^{1}H} NMR (C_6D_6): 25 (s, *C*H$_3$), 26 (s, *C*H$_3$), 50 (s, *C*HMe$_2$), 109 (s, *C*HAr), 121 (s, *C*HAr), 122 (s, *C*Ar), 127 (s, *C*HAr), 138 (s, *C*Ar), 145 (s, *C*Ar). IR: 2725(16), 1708(16), 1586(14), 1558(3), 1316(3), 1292-(1), 1242(11), 1162(6), 1134(4), 1106(8), 1072(5), 1045(9), 958-(10), 944(8), 930(10), 873(13), 854(13), 808(3), 780(12), 762(7), 753(2), 740(7), 630(15). Anal. Calcd for $C_{16}H_{20}N_2SbCl$: C 48.34, H 5.07, N 7.05; Found: C 47.77, H 5.47, N 6.68.

ClSb(PhN)$_2$C$_{10}$H$_6$ (9f). Yellow−orange, fibrous crystals of **9f** (0.413 g, 67%) were obtained overnight by recrystallization from a 50:50 toluene/hexane mixture at −20 °C. The crystals were not suitable for X-ray diffraction. ^{1}H NMR (CD_2Cl_2): 6.5 (dd, $^3J_{HH}$ = 8 Hz, $^4J_{HH}$ = 1 Hz, 2H, *H*Ar), 7.2 (t, $^3J_{HH}$ = 8 Hz, 2H, *H*Ar), 7.3 (d, $^3J_{HH}$ = 8 Hz, 6H, *H*Ar), 7.46−7.52 (m, 4H, *H*Ar). ^{13}C{^{1}H} NMR (CD_2Cl_2): 112 (s, *C*HAr), 119 (s, *C*Ar), 121 (s, *C*HAr), 126.8 (s, *C*HAr), 127.1 (s, *C*HAr), 128 (s, *C*HAr), 131 (s, *C*HAr), 138 (s, *C*Ar), 145.5 (s, *C*Ar), 146.0 (s, *C*Ar). IR: 1590(12), 1578(15), 1557(4), 1484(7), 1344(15), 1283(7), 1272(8), 1257(9), 1205(11), 1166(13), 1037(5), 1025(12), 915(10), 876(14), 810(3), 797(11), 757(1), 739(6), 695(2). Anal. Calcd for $C_{22}H_{16}N_2SbCl$: C 56.75, H 3.46, N 6.02; Found: C 56.46, H 3.99, N 5.84.

General Procedure for the Preparation of Pnictogenium Gallate Salts 10a−d. To a solution of the appropriate diamidochloropnictine **9a−d** (0.2 − 0.3 g) in 5 mL of toluene was added a solution of $GaCl_3$ (1 equiv) in 5 mL of toluene, causing immediate precipitation of the corresponding pnictogenium gallate salt as a powder. The solvent was removed by decantation, and the solid was washed with 2 × 5 mL portions of hexane and then dried under vacuum to yield **10a−d**.

[P(*i*PrN)$_2$C$_{10}$H$_6$]GaCl$_4$ (10a). The gallate salt **10a** was obtained as a dark purple powder (0.276 g, 86%). X-ray quality crystals were obtained by placing a concentrated CH_2Cl_2 solution of **10a** in the freezer at −20 °C for 1 week. ^{1}H NMR (CD_2Cl_2): 1.7 (dd, $^3J_{HH}$ = 7 Hz, $^4J_{PH}$ = 3 Hz, 12H, C*H*$_3$) 4.5 (doublet of septets, $^3J_{PH}$ = 11 Hz, $^3J_{HH}$ = 7 Hz, 2H, C*H*Me$_2$), 6.9 (d, $^3J_{HH}$ = 8 Hz, 2H, *H*Ar), 7.4 (t, $^3J_{HH}$ = 8 Hz, 2H, *H*Ar), 7.6 (d, $^3J_{HH}$ = 8 Hz, 2H, *H*Ar). ^{13}C{^{1}H} NMR (CD_2Cl_2): 23 (d, $^3J_{PC}$ = 19 Hz, *C*H$_3$), 56 (d, $^2J_{PC}$ = 22 Hz, *C*HMe$_2$), 111 (d, $^3J_{PC}$ = 3 Hz, *C*HAr), 124 (d, $^3J_{PC}$ = 5 Hz, *C*Ar), 127 (s, *C*HAr), 128 (s, *C*HAr), 134 (d, $^2J_{PC}$ = 8 Hz, *C*Ar), 137 (s, *C*Ar). ^{31}P{^{1}H} NMR (CD_2Cl_2): 239 (s). IR: 1626-(14), 1606(17), 1577(9), 1316(12), 1294(6), 1252(16), 1178(8), 1145(4), 1111(7), 1076(5), 1054(11), 1047(10), 1019(3), 975(15), 943(17), 918(13), 819(2), 809(6), 762(1), 621(12). Anal. Calcd for $C_{16}H_{20}N_2PCl_4Ga$: C 39.80, H 4.17, N 5.80; Found: C 40.22, H 4.52, N 5.86.

[P(PhN)$_2$C$_{10}$H$_6$]GaCl$_4$ (10b). The gallate salt **10b** was obtained as a brown powder (0.434 g, 98%). X-ray quality crystals were obtained by placing a concentrated CH_2Cl_2 solution of **10b** in the freezer at −20 °C for 1 week. ^{1}H NMR (CD_2Cl_2): 6.2 (broad s, 2H, *H*Ar), 7.2 (broad s, 2H, *H*Ar), 7.5 (broad s, 2H, *H*Ar), 7.7 (broad s, 10H, *H*Ar). ^{13}C{^{1}H} NMR: the fluxionality of this compound, combined with its low solubility, prevented collection of a ^{13}C NMR spectrum with a good enough signal-to-noise ratio to report a listing of peaks. ^{31}P{^{1}H} NMR (CD_2Cl_2): 195 (broad singlet). IR: 1630(15), 1598(11), 1588(10), 1576(6), 1485(6), 1290-(13), 1271(10), 1219(12), 1196(8), 1165(7), 1130(6), 1107(8), 1075-(5), 1040(4), 999(10), 857(15), 845(14), 820(3), 754(2), 693(1), 545(7), 526(14), 513(9). Anal. Calcd for $C_{22}H_{16}N_2PCl_4Ga$: C 47.97, H 2.93, N 5.09; Found: C 47.76, H 3.26, N 5.09.

[As(*i*PrN)$_2$C$_{10}$H$_6$]GaCl$_4$ (10c). The gallate salt **10c** was obtained as a dark blue powder. As much of the solid as possible was dissolved in 15 mL of CH_2Cl_2, and the solution was filtered and placed in the freezer at −20 °C to yield dark blue crystals of **10c** after 1 week (0.17 g, 37%). X-ray quality crystals were obtained by dissolving a very small amount of **10c** in toluene and placing the solution in the freezer (−20 °C) for 2 weeks. ^{1}H NMR (CD_2Cl_2): 1.7 (d, $^3J_{HH}$ = 4 Hz, 12H, C*H*$_3$) 4.5 (broad, 2H, C*H*Me$_2$), 6.7 (broad, 2H, *H*Ar), 7.3 (broad, 4H, *H*Ar). ^{13}C{^{1}H} NMR: the fluxionality of this compound, combined with its low solubility, prevented collection of a ^{13}C NMR spectrum with a good enough signal-to-noise ratio to report a listing of peaks. IR: 2725(13), 2670-(14), 1618(18), 1569(12), 1311(5), 1284(3), 1215(15), 1169(11), 1138(6), 1111(8), 1067(9), 1049(17), 961(10), 937(7), 811(4), 786-(13), 777(16), 754(2), 734(1), 697(18), 613(14). Anal. Calcd for

$C_{16}H_{20}N_2AsCl_4Ga$: C 36.48, H 3.83, N 5.32; Found: C 36.37, H 4.13, N 5.28.

[As(PhN)$_2$C$_{10}$H$_6$]GaCl$_4$ (10d). The gallate salt **10d** was obtained a purple powder (0.352 g, 83%). X-ray quality crystals were obtained by placing a concentrated CH_2Cl_2 solution of **10d** in the freezer at −20 °C for 1 week. ^{1}H NMR (CD_2Cl_2): one broad peak in aryl region from 7.4 to 7.9 ppm. ^{13}C{^{1}H} NMR: the fluxionality of this compound, combined with its low solubility, prevented collection of a ^{13}C NMR spectrum with a good enough signal-to-noise ratio to report a listing of peaks. IR: 1619(13), 1589(12), 1569(8), 1482(6), 1341(13), 1285(14), 1272(8), 1223(16), 1200-(12), 1167(10), 1125(11), 1073(14), 1046(4), 1025(15), 1003(15), 959(5), 819(2), 807(8), 768(7), 763(6), 757(9), 748(3), 693(1). Calcd for $C_{22}H_{16}N_2AsCl_4Ga$: C 44.42, H 2.71, N 4.71; Found: C 44.10, H 2.59, N 4.50.

Preparation of [P(*i*PrN)$_2$C$_{10}$H$_6$]OTf (11a). ClP(*i*PrN)$_2$C$_{10}$H$_6$ (**9a**) (0.298 g, 0.97 mmol) and $AgSO_3CF_3$ (0.275 g, 1.1 mmol) were weighed in the same vial. and 10 mL of toluene was added to the solid mixture. After 1 h of stirring, the reaction mixture was filtered through a glass frit packed with Celite. The filtrate was concentrated and placed in the freezer at −20 °C overnight to yield bright red crystals of **11a** (0.274 g, 67%). The crystals were not suitable for X-ray diffraction. ^{1}H NMR (C_6D_6): 1.2 (dd, $^3J_{HH}$ = 7 Hz, $^4J_{PH}$ = 2 Hz, 12H, C*H*$_3$) 3.8 (doublet of septets, $^3J_{PH}$ = 14 Hz, $^3J_{HH}$ = 7 Hz, 2H, C*H*Me$_2$), 6.4 (d, $^3J_{HH}$ = 8 Hz, 2H, *H*Ar), 7.1 (t, $^3J_{HH}$ = 8 Hz, 2H, *H*Ar), 7.2 (d, $^3J_{HH}$ = 8 Hz, 2H, *H*Ar) ^{13}C{^{1}H} NMR (C_6D_6): 22 (d, $^3J_{PC}$ = 19 Hz, *C*H$_3$), 52 (d, $^2J_{PC}$ = 28 Hz, *C*HMe$_2$), 110 (d, $^3J_{PC}$ = 2 Hz, *C*HAr), 120 (d, $^3J_{PC}$ = 3 Hz, *C*Ar), 120 (q, $^1J_{FC}$ = 319 Hz, *C*F$_3$), 123 (s, *C*HAr), 127 (s, *C*HAr), 136 (d, $^2J_{PC}$ = 5 Hz, *C*Ar), 137 (s, *C*Ar). ^{31}P{^{1}H} NMR (C_6D_6): 142 (s). ^{19}F NMR (CH_2Cl_2): −78.3 (s). IR: 1625(17), 1577(5), 1391(10), 1324-(15), 1291(7), 1232(7), 1213(8), 1193(11), 1173(8), 1145(9), 1133-(12), 1114(13), 1075(13), 1013(6), 947(16), 916(16), 819(4), 810(11), 767(3), 635(1), 572(14), 559(13), 515(2). Anal. Calcd for $C_{17}H_{20}N_2O_3F_3PS$: C 48.57, H 4.80, N 6.66; Found: C 48.30, H 5.12, N 6.57.

Preparation of [P(PhN)$_2$C$_{10}$H$_6$]OTf (11b). ClP(PhN)$_2$C$_{10}$H$_6$ (**9b**) (0.300 g, 0.80 mmol) and $AgSO_3CF_3$ (0.226 g, 0.88 mmol) were weighed in the same vial, and 15 mL of toluene was added to the solid mixture. After 3 h of stirring, the reaction mixture was filtered through a glass frit packed with Celite. The filtrate was concentrated and placed in the freezer at −20 °C overnight to yield bright red crystals of **11b** (0.182 g, 47%). ^{1}H NMR (C_6D_6): 6.4 (d, $^3J_{HH}$ = 5 Hz, 2H, *H*Ar), 6.9 (t, $^3J_{HH}$ = 5 Hz, 2H, *H*Ar), 7.0 (m, 2H, *H*Ar), 7.07 (t, $^3J_{HH}$ = 5 Hz, 4H, *H*Ar), 7.14 (d, $^3J_{HH}$ = 5 Hz, 2H, *H*Ar), 7.4 (d, $^3J_{HH}$ = 5 Hz, 4H, *H*Ar). ^{13}C{^{1}H} NMR (C_6D_6): 112 (s, *C*HAr), 119 (s, *C*Ar), 120 (q, $^1J_{FC}$ = 320 Hz, *C*F$_3$), 123 (s, *C*HAr), 127 (s, *C*HAr), 128.7 (s, *C*HAr), 129.2 (s, *C*HAr), 130 (d, $^3J_{PC}$ = 7 Hz, *C*HAr), 131 (s, *C*HAr), 136 (s, *C*Ar), 138 (d, $^2J_{PC}$ = 5 Hz, *C*Ar), 140 (d, $^2J_{PC}$ = 23 Hz, *C*Ar). ^{31}P{^{1}H} NMR (C_6D_6): 118 (s). ^{19}F NMR (CH_2Cl_2): −78.6 (s). IR: 1630(16), 1601(15), 1576(5), 1490(6), 1334(16), 1282(6), 1224(6), 1176(9), 1156(6), 1130(10), 1108(7), 1075(8), 1022(5), 997(12), 972(14), 848(17), 832(17), 814(4), 763(11), 754(2), 696(1), 637(3), 608(14), 547-(13). Anal. Calcd for $C_{23}H_{16}N_2O_3F_3PS$: C 56.56, H 3.30, N 5.74; Found: C 55.70, H 3.43, N 5.53.

Preparation of (NMe$_2$)Sb(*i*PrN)$_2$C$_{10}$H$_6$ (14). A Schlenk flask containing a solution of tris(dimethylamido)antimony (2.10 g, 8.3 mmol) in 30 mL of toluene was cooled in a dry ice/acetone bath to −78 °C. A solution of 1,8-(*i*PrNH)$_2$C$_{10}$H$_6$ (2.00 g, 8.3 mmol) in 10 mL of toluene was transferred into the flask via cannula, producing a purple solution. The reaction mixture was stirred at low temperature for an additional 30 min and then slowly allowed to warm to room temperature, during which time the reaction mixture turned from purple to orange, and NH(CH$_3$)$_2$ gas evolved. After stirring for an additional 2 h, all volatiles were removed to give an orange oil. The oil was dissolved in a 50:50 toluene/hexane mixture and placed in the freezer at −20 °C overnight to yield yellow crystals of **14** (1.82 g, 54%). ^{1}H NMR (C_6D_6): 1.2 (d, $^3J_{HH}$ = 7 Hz, 6H, C*H*$_3$), 1.3 (d, $^3J_{HH}$ = 7 Hz, 6H, C*H*$_3$), 2.4 (s, 6H, NC*H*$_3$), 4.1 (septet, $^3J_{HH}$ = 6 Hz, 2H, C*H*Me$_2$), 6.7 (t, $^3J_{HH}$ = 5 Hz, 2H, *H*Ar), 7.3 (d, $^3J_{HH}$ = 5 Hz, 4H, *H*Ar). ^{13}C{^{1}H} NMR (C_6D_6): 25 (s, *C*H$_3$), 26 (s, *C*H$_3$), 42 (s, NCH$_3$), 50 (s, *C*HMe$_2$), 107 (s, *C*HAr), 119 (s, *C*HAr), 122 (s, *C*Ar), 127 (s, *C*HAr), 138 (s, *C*Ar), 148 (s, *C*Ar). IR : 2373(16), 1893(17), 1692(18), 1563(1), 1387(2), 1321-(3), 1296(4), 1171(5), 1138(5), 1108(9), 1073(6), 1047(10), 930-(8), 868(12), 807(9), 781(11), 762(9), 748(7), 641(15), 631(14), 554(13). Anal. Calcd for $C_{18}H_{26}N_3Sb$: C 53.23, H 6.45, N 10.35; Found: C 53.44, H 6.33, N 10.03.

Preparation of [Sb(*i*PrN)$_2$C$_{10}$H$_6$·NHMe$_2$]OTf (15). A Schlenk flask containing a solution of (NMe$_2$)Sb(*i*PrN)$_2$C$_{10}$H$_6$ (**14**) (0.50 g, 1.2 mmol) in 20 mL of toluene was cooled in a dry ice/acetone bath to −78 °C. A solution of triflic acid (0.11 mL, 1.2 mmol) in 5 mL of toluene was transferred into the flask via cannula, causing an immediate color change from light to dark orange. The reaction mixture was stirred at low temperature for an additional 20 min, during which time a yellow solid precipitated. As the reaction warmed to room temperature, the solid dissolved, returning the reaction mixture to dark orange. All volatiles were removed, resulting in an orange oil. The oil was dissolved in a 50:50 toluene/hexane mixture and placed in the freezer at −20 °C overnight to yield yellow crystals of **15** (0.47 g, 68%). ^{1}H NMR (C_6D_6): 1.4 (broad, 12H, C*H*$_3$), 1.9 (s, 6H, NC*H*$_3$), 4.0 (septet, $^3J_{HH}$ = 6 Hz, 2H, C*H*Me$_2$), 6.3 (broad, 1H, N*H*), 6.5 (d, $^3J_{HH}$ = 8 Hz, 2H, *H*Ar), 7.1 (t, $^3J_{HH}$ = 8 Hz, 2H, *H*Ar), 7.2 (d, $^3J_{HH}$ = 8 Hz, 2H, *H*Ar). ^{13}C{^{1}H} NMR (C_6D_6): 25 (s, *C*H$_3$), 38 (s, NCH$_3$), 53 (s, *C*HMe$_2$), 110 (s, *C*HAr), 121.2 (s, *C*HAr), 121.5 (s, *C*Ar), 122 (q, $^1J_{FC}$ = 320 Hz, *C*F$_3$), 127 (s, *C*HAr), 138 (s, *C*Ar), 145 (s, *C*Ar). ^{19}F NMR (CH_2Cl_2): −78.8 (s).IR : 3167(19), 1912(14), 1832(17), 1807-(16), 1723(15), 1603(11), 1559(1), 1510(12), 1405(18), 1329(9), 1317(8), 1291(7), 1218(6), 1113(6), 1158(6), 1062(5), 1021(4), 961-(5), 943(6), 930(7), 876(4), 812(3), 780(10), 757(2), 636(8), 574-(13). Anal. Calcd for $C_{19}H_{27}N_3O_3F_3SSb$: C 41.02, H 4.89, N 7.55; Found: C 40.45, H 4.54, N 7.27.

Results and Discussion

The diamidochloropnictines ClPn(RN)$_2$C$_{10}$H$_6$ (**9a**−**f**) serve as precursors for pnictogenium cation synthesis and are readily available from the dehydrohalide coupling reactions of *N*,*N*′-diisopropyl-1,8-diaminonaphthalene or *N*,*N*′-diphenyl-1,8-diaminonaphthalene with the appropriate pnictogen trichloride (eq 1). Triethylamine was used as an acid scavenger in all reactions, and the colorless diamidochlorophosphines (**9a**,**b**), yellow diamidochloroarsines (**9c**,**d**), and orange diamidochlorostibines (**9e**−**f**) were obtained in good yields after stirring for 4 days at room temperature. Formation of the diamidochloropnictines was accompanied by a loss of symmetry for the bis(amido)-naphthalene framework in the ^{1}H NMR spectra, which show two distinct sets of resonances for the N-bound substituents as expected for these rigid pyramidal species. For example, the NMR spectra of the *i*Pr compounds display two inequivalent methyl groups, which are coupled to the methine CH groups, and in the case of **9a** with phosphorus. The structural details of **9a**−**c** and **9e** were further confirmed by single-crystal X-ray analyses. Crystallographic data are listed in Table 1, and structural views of **9a**,**c**,**e** are presented in Figure 1. Selected structural parameters and ^{31}P NMR chemical shifts are detailed in Table 3.

The solid-state structures of ClP(*i*PrN)$_2$C$_{10}$H$_6$ (**9a**) and ClP-(PhN)$_2$C$_{10}$H$_6$ (**9b**)[22] exhibit nearly identical bond lengths and

(22) Thermal ellipsoid plot for this compound is provided in the Supporting Information.

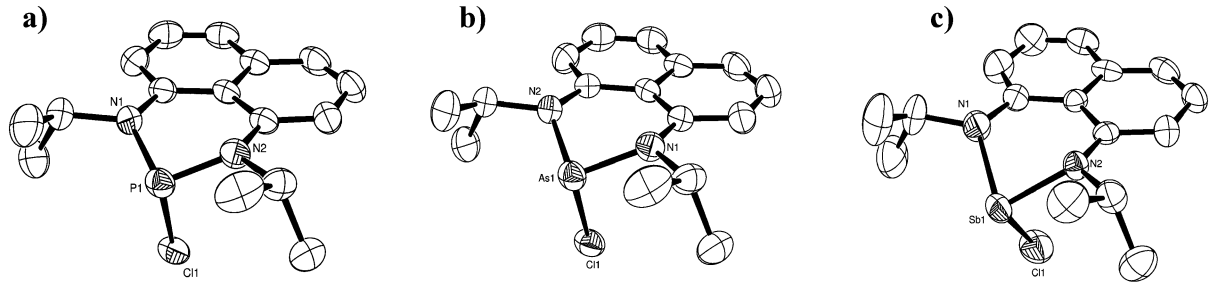

Figure 1. Thermal ellipsoid plots showing the molecular structures and partial atom numbering schemes for (a) $ClP(^{i}PrN)_2C_{10}H_6$ (**9a**), (b) $ClAs(^{i}PrN)_2C_{10}H_6$ (**9c**), and (c) $ClSb(^{i}PrN)_2C_{10}H_6$ (**9e**).[27] Hydrogen atoms have been omitted for clarity.

angles. Both compounds have relatively short P−Cl bonds (**9a** P−Cl = 2.1723(9) Å; **9b** 2.148(1) Å), which are only slightly longer than the P−Cl bond distance observed in phosphorus trichloride (2.04 Å).[23] There is no evidence for spontaneous P−Cl bond heterolysis in solution to generate the corresponding phosphenium cations, and the ^{31}P NMR chemical shifts of **9a** (δ ^{31}P = 102 ppm) and **9b** (δ ^{31}P = 99 ppm) are similar to those reported for other diamidochlorophosphines.[24] Both species have pyramidal phosphorus centers (Σ P angles **9a** = 300.5-(1)°; **9b** = 301.2(1)°) that are out of the plane formed by the bis(amido)naphthalene ligand (bend angle **9a** = 31.7°; **9b** = 32.1°).[25] Nevertheless, the P−N bond lengths in **9a** (P−N(1) = P−N(2) = 1.670(2) Å) and **9b** (P−N(1) = 1.678(2) Å; P−N(2) = 1.681(2) Å) are shorter than the benchmark P−N single bond (1.800(4) Å)[26] observed in $H_3NPO_3^-$, indicating that some degree of N−P π-overlap is present in these compounds.

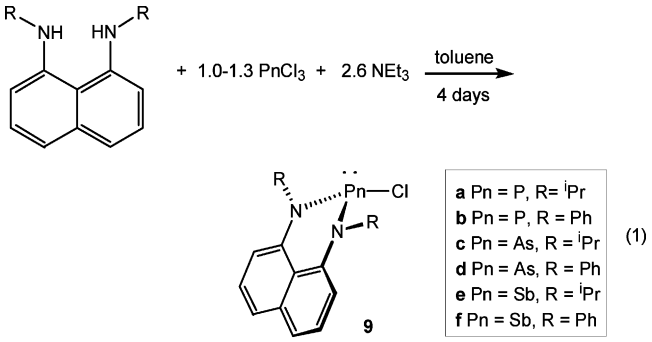

(1)

The diamidochloroarsine $ClAs(^{i}PrN)_2C_{10}H_6$ (**9c**) and the diamidochlorostibine $ClSb(^{i}PrN)_2C_{10}H_6$ (**9e**)[27] are structurally similar to the analoguous phosphine **9a**; however, with the increasing size of the pnictogen center, the N(1)−Pn−N(2) angle (P 99.7(1)°; As 95.61(9)°; Sb 86.5(2)°) becomes more acute, and the Pn−Cl moiety moves further out of the plane of the bis(amido)naphthalene ligand (bend angle: P 31.7°; As 31.9°; Sb 39.6°). The As−N bonds in **9c** (As−N(1) = 1.810(2) Å; As−N(2) = 1.812(2) Å) lie at the lower end of the known range of As−N bond distances in diamidochloroarsines (1.84 ± 0.04 Å)[8] and compare well with those in 2-chloro-1,3-di-*t*-butyl-1,3,2-diazaarsolene (**2-Cl**, R= ^{t}Bu, Pn =As; As−N = 1.8045(12), 1.8057(12) Å).[11b] Similarly, the Sb−N bonds in **9e** (Sb−N(1) = 2.021(5) Å; Sb−N(2) = 2.017(4) Å) are relatively short and comparable to those in 2-chloro-1,3-di-*t*-butyl-1,3,2-diazastibolene (**2-Cl**, R = ^{t}Bu, Pn =Sb; Sb−N = 1.998(4), 2.000(4) Å)[11b] and in cyclo-$[Me_2Si(N^{t}Bu)_2SbCl]$ (**3-Cl**, R = ^{t}Bu, Pn = Sb; Sb−N = 1.995(5) Å).[12]

In a series of diamidochloropnictines reported by Gudat and co-workers (**2-Cl**, R = ^{t}Bu, Pn = P, As, Sb), the Pn−Cl bonds in the compounds actually decrease in length with an increase in the size of the pnictogen atom (P−Cl = 2.6915(4) Å; As−Cl = 2.6527(4) Å; Sb−Cl 2.6460(15) Å).[11b] While this trend is counter to that expected based on the respective atomic radii of the atoms, it was justified by suggesting that the stibenium cation is the best chloride acceptor of the series, while the phosphenium cation is the poorest. The reverse trend is observed in the diamidonaphthalene-based series $ClPn(^{i}PrN)_2C_{10}H_6$ (**9a**,**c**,**e**), where the Pn−Cl bond lengths increase with the size of the pnictogen atom (P−Cl = 2.1723(9) Å; As−Cl = 2.2820(8) Å; Sb−Cl = 2.392(2) Å). Combining this observation with the previous explanation leads to a reversal of the chloride acceptor ordering in this series with the stibenium cation as the poorest chloride acceptor, while the phosphenium cation appears to be the better chloride acceptor. As discussed next, this proposition contradicts the respective reactivities of the diamidochloropnictines, $ClPn(RN)_2C_{10}H_6$ (**9a**−**f**). Also of note, the Sb atoms in the 1,3,2-diazastibolene (**2-Cl**, R = ^{t}Bu, Pn = Sb) display intermolecular contacts between the Sb center and the halogen atom of a neighboring molecule, forming zigzag chains of pairs of Sb and Cl atoms in the solid state. No intermolecular contacts within the sum of the van der Waals radii are present to the Sb atom in $ClSb(^{i}PrN)_2C_{10}H_6$ (**9e**).

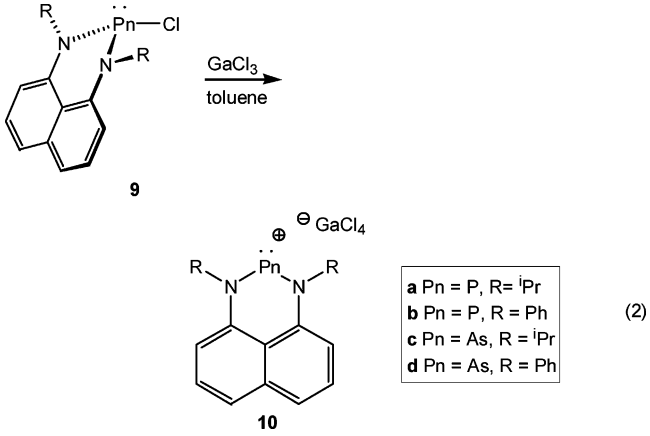

(2)

The phosphenium salts $[P(RN)_2C_{10}H_6][GaCl_4]$ (**10a**,**b**) and arsenium salts $[As(RN)_2C_{10}H_6][GaCl_4]$ (**10c**,**d**) are readily accessible from pnictogen−chlorine bond heterolysis of **9a**−**d**

(23) Corbridge, D. E. C. *The Structural Chemistry of Phosphorus*; Elsevier: Amsterdam, 1974.

(24) Burford, N.; Cameron, T. S.; Conroy, K. D.; Ellis, B.; MacDonald, C. L. B.; Ovans, R.; Phillips, A. D.; Ragogna, P. J.; Walsh, D. *Can. J. Chem.* **2002**, *80*, 1404.

(25) Bend angle is measured between the plane of the naphthalene group and the N−Pn−N plane.

(26) Cameron, T. S.; Chan, C.; Chute, W. J. *Acta Crystallogr., Sect. B: Struct. Sci.* **1980**, *36*, 2391.

(27) For simplicity, discussion has been limited to only one of the two independent units of **9e** in the unit cell. There are no significant differences in the bond lengths and angles between these two species.

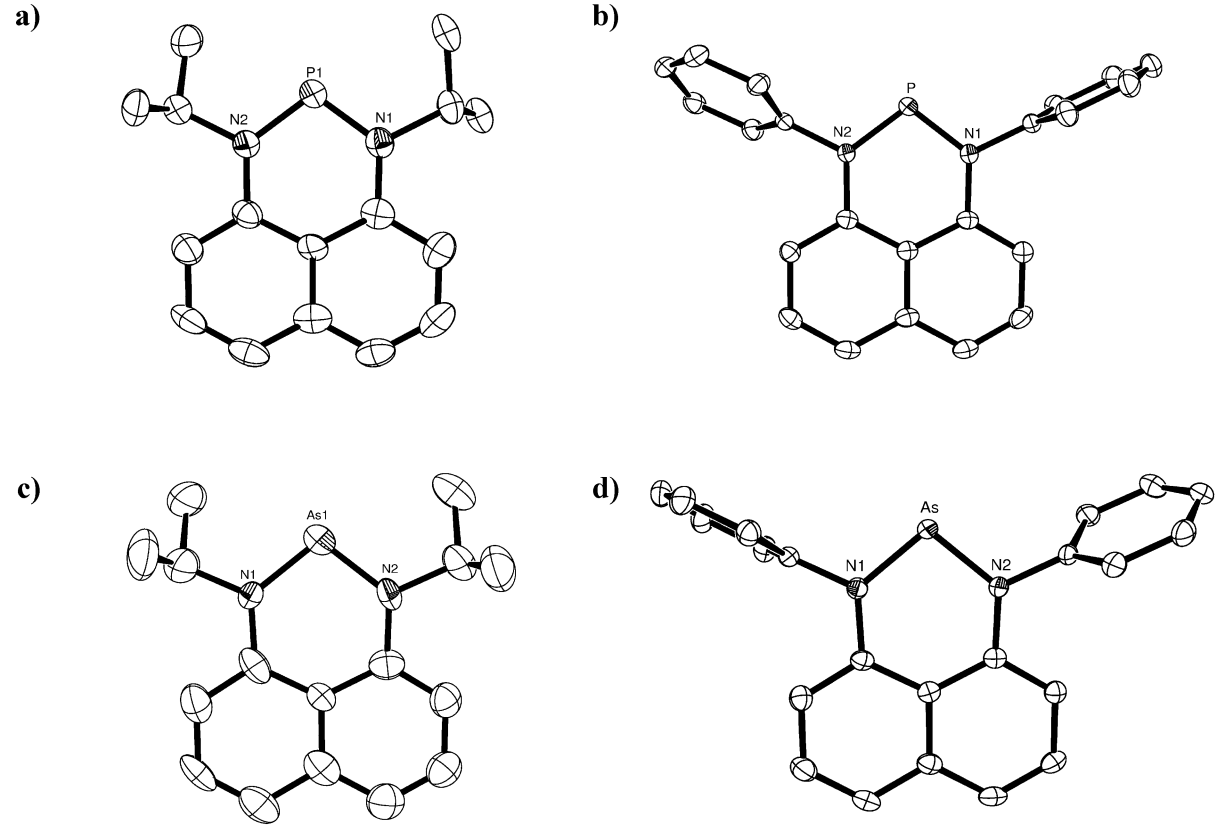

Figure 2. Thermal ellipsoid plot showing the molecular structures and partial atom numbering schemes for the phosphenium cations in (a) $[P(^iPrN)_2C_{10}H_6]GaCl_4$ (**10a**) and (b) $[P(PhN)_2C_{10}H_6]GaCl_4$ (**10b**) and arsenium cations in (c) $[As(^iPrN)_2C_{10}H_6]GaCl_4$ (**10c**) and (d) $[As(PhN)_2C_{10}H_6]GaCl_4$ (**10d**). $GaCl_4^-$ anions and H atoms have been omitted for clarity.

using gallium trichloride (eq 2). Addition of $GaCl_3$ to a toluene solution of $ClP(^iPrN)_2C_{10}H_6$ (**9a**) or $ClP(PhN)_2C_{10}H_6$ (**9b**) caused immediate precipitation of a dark purple (**10a**) or brown solid (**10b**), which when dissolved in CH_2Cl_2 exhibited ^{31}P NMR chemical shifts of 235 and 195 ppm, respectively. These values are similar to those reported for other N-heterocyclic phosphenium cations.[4] Similarly, the addition of $GaCl_3$ to toluene solutions of $ClAs(^iPrN)_2C_{10}H_6$ (**9c**) and $ClAs(PhN)_2C_{10}H_6$ (**9d**) resulted in immediate precipitation of the respective arsenium salts, $[As(^iPrN)_2C_{10}H_6][GaCl_4]$ (**10c**) and $[As(PhN)_2C_{10}H_6][GaCl_4]$ (**10d**), as dark blue and purple solids, respectively. The arsenium salts are somewhat more soluble than their phosphenium counterparts, and **10c** can be recrystallized from toluene.

Toluene solutions of the phosphines **9a**,**b** also react rapidly with 1 equiv of silver triflate (AgOTf, OTf = triflate or $CF_3SO_3^-$) to generate the triflate salts $[P(^iPrN)_2C_{10}H_6][OTf]$ (**11a**) and $[P(PhN)_2C_{10}H_6][OTf]$ (**11b**). The dark red compounds are soluble in arene solvents and have ^{31}P NMR chemical shifts of 142 ppm (**11a**) and 119 ppm (**11b**) in C_6D_6. The ^{31}P NMR resonances of **11a** (179 ppm) and **11b** (130 ppm) appear at lower fields in CD_2Cl_2, suggesting that significant contact occurs between the phosphorus cations and the triflate anions in less polar solvents. In contrast, the diamidochloroarsines **9c**,**d** are slow to react with both silver triflate and trimethylsilyltriflate, and the reactions produced mixtures of products that could not be separated. Reaction of **9c** with silver tetrafluoroborate also produced multiple products, but purple crystals of the tetrafluoroborate salt $[As(^iPrN)_2C_{10}H_6][BF_4]$ (**12**) could be isolated from the reaction mixture.

Unexpectedly, the addition of $GaCl_3$ or $AlCl_3$ to toluene solutions of the diamidochlorostibine species **9e**,**f** resulted in the precipitation of metallic antimony from the reaction, even at low temperatures. Trimethylsilyltriflate did not react with **9e** at room temperature, and heating **9e** with Me_3SiOTf in toluene at 100 °C for 12 h produced a mixture of products that could not be separated. Attempts to prepare the desired stibenium cations with the silver salts AgOTf and $AgBF_4$ were also unsuccessful.

The cations in salts **10a**−**d** represent rare examples of six-membered N-heterocyclic phosphenium and arsenium cations possessing π-conjugated carbon backbones.[17] The solid-state structures of the pnictogenium salts $[Pn(RN)_2C_{10}H_6][GaCl_4]$ **10a**,**b** (Pn = P, R = ^{i}Pr, Ph) and **10c**,**d** (Pn = As, R = ^{i}Pr, Ph) were determined by X-ray crystallography, and the respective cations are depicted in Figure 2. Crystallographic data are listed in Table 2, and selected structural parameters and ^{31}P NMR chemical shifts are detailed in Table 3. In $[P(^iPrN)_2C_{10}H_6][GaCl_4]$ (**10a**), the closest contacts between the dicoordinate phosphorus atom and the chlorine atoms of the anion are greater than 4 Å in length, well outside the sum of the van der Waals radii for phosphorus and chlorine (3.6 Å).[28] The gallate anion is in closer proximity to the phosphenium cation in $[P(PhN)_2C_{10}H_6][GaCl_4]$ (**10b**), with the shortest P−Cl contact being 3.258(7) Å. This difference in cation−anion interaction is likely a result of the less basic aryl substituted ligand framework of **10b**, which should provide less effective stabilization of the low-coordinate, cationic phosphorus center. Similar features were observed with the arsenium cations: the ion pair is further separated in $[As(^iPrN)_2C_{10}H_6][GaCl_4]$ (**10c**) (closest As−Cl contact 3.49(1) Å) than in the aryl substituted analogue $[As(PhN)_2C_{10}H_6][GaCl_4]$ (**10d**) (As−Cl = 3.201(6) Å). The closer approach of the gallate anions to the arsenium cations (**10c**,**d**)

(28) Bondi, A. *J. Phys. Chem.* **1964**, *68*, 441.

as compared to the phosphenium cations (**10a**,**b**) can be accounted for by the less effective π-overlap between As and N, as compared to P and N, leaving the arsenic centers in **10c**,**d** more electron deficient than the corresponding phosphorus centers in **10a**,**b**.

Structural features that are associated with the formation of the pnictogenium cations are a contraction of the Pn−N bonds and the formation of a more planar heterocyclic framework, indicating the presence of increased Pn−N π-bonding in the coordinatively unsaturated species. The P−N bonds in the phosphenium salts $[P(^{i}PrN)_2C_{10}H_6]GaCl_4$ (**10a**) (P−N(1) = 1.609(8) Å; P−N(2) = 1.629(7) Å) and $[P(PhN)_2C_{10}H_6]GaCl_4$ (**10b**) (P−N(1) = 1.633(2) Å; P−N(2) = 1.634(2) Å) are shorter than those in the respective phosphines **9a** (P−N(1) = P−N(2) = 1.670(2) Å) and **9b** (P−N(1) =1.678(2) Å; P−N(2) = 1.681-(2) Å) and those in the five-membered aromatic phosphenium cation **2** (R = ^{t}Bu, Pn = P; P−N = 1.660(2)Å).[29] The decrease of the P−N bonds in **10a**,**b** is not accompanied by any significant changes in the N−C and C−C bonds in the PN_2C_3 heterocyclic ring (Table 3), but the N(1)−P−N(2) angles in the phosphenium cations (**10a** 105.4(3)°; **10b** 103.17(8)°) are several degrees wider than those in the corresponding chlorophosphines (**9a** 99.7(1)°; **9b** 98.9(1)°), perhaps reflecting a modified hybridization (sp^2 vs sp^3) of the dicoordinate phosphorus atoms. The *N*-isopropyl substituted phosphenium cation **10a** is essentially planar (bend angle = 2.2°), while the *N*-phenyl substituted compound is slightly distorted from planarity (bend angle = 5.5°). This is likely only a consequence of crystal packing as all of the other metrical parameters in the two structures are nearly identical. The structure of the phophenium triflate salt $[P(PhN)_2C_{10}H_6]OTf$ (**11b**) was also determined by X-ray crystallography and demonstrates that the identity of the anion does not greatly affect the structural features of the corresponding cation.[22] The phosphenium cation in the triflate salt (**11b**) is essentially identical to that in the gallate salt (**10b**) and actually exhibits a greater degree of planarity (bend angle = 4.0°) despite the closer approach of the triflate anion to the low-coordinate phosphorus center (P−O = 2.594(5) Å).

Likewise, the As−N bonds in the arsenium salts $[As(^{i}PrN)_2C_{10}H_6]GaCl_4$ (**10c**) (As−N(1) = 1.762(7) Å; As−N(2) = 1.757(7) Å) and $[As(PhN)_2C_{10}H_6]GaCl_4$ (**10d**) (As−N(1) = 1.771(3) Å; As−N(2) = 1.765(3) Å) are shorter than those in the starting arsine **9c** (As−N(1) = 1.810(2) Å; As−N(2) = 1.812(2) Å) and those in the five-membered aromatic arsenium cation **2** (R = ^{t}Bu, Pn = As; As−N = 1.8377(14), 1.8271(13) Å).[11b] This suggests that the bis(amido)naphthalene frameworks are more electron-rich than the corresponding bis(amido)alkene frameworks; however, it could also be a consequence of a change in ring size. Like the phosphorus analogues, the *N*-isopropyl substituted arsenium cation **10c** exhibits a greater degree of planarity (bend angle = 3.9°) than its *N*-phenyl substituted counterpart **10d** (bend angle = 6.4°).

The inability to generate the stibenium analogue of **10a**−**d** using halide abstraction reactions of **9e**,**f** with Lewis acids such as $GaCl_3$, $AlCl_3$, Me_3SiOTf, or silver salts prompted the exploration of an alternative synthetic strategy summarized in eq 3.[13b] For the transamination reaction, $Sb(NMe_2)_3$ and 1,8-bis(isopropylamino)naphthalene were combined at −78 °C and then slowly allowed to warm to room temperature. During this reaction, the initial purple solution gradually turned orange, and evolution of $NHMe_2$ gas was apparent. The new heteroleptic triamidostibene, $(Me_2N)Sb(^{i}PrN)_2C_{10}H_6$ (**14**) was isolated in good yield as a yellow crystalline solid. Like the chloro analogue **9e**, the ^{1}H NMR spectrum of **14** exhibited two signals for the ^{i}Pr methyl groups consistent with the proposed pyramidal Sb center. The structural details of **14** were further confirmed with single-crystal X-ray analysis, and the results are shown in Figure 3. Compound **14** exhibits nearly identical metrical parameters to those observed in the structure of **9e**, with the Sb−Cl group replaced with an Sb−NMe_2 bond (Sb−N(3) = 2.056(4) Å) (Table 3). Compounds **9e**,**f** and **14** represent the first reported examples of six-membered N-heterocyclic stibines.

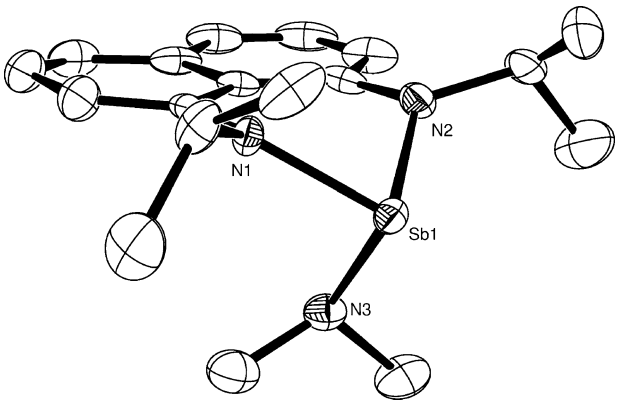

Figure 3. Thermal ellipsoid plot showing the molecular structure and partial atom numbering scheme of $(Me_2N)Sb(^{i}PrN)_2C_{10}H_6$ (**14**). H atoms have been omitted for clarity.

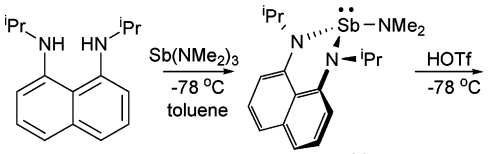

14

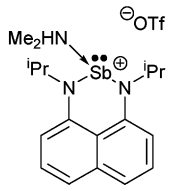

15 (3)

We anticipated that the addition of triflic acid (HOTf) to **14** would protonate the dimethylamido group, liberate $NHMe_2$, and generate a stibenium triflate salt; however, no gas evolution was observed in the reaction of **9** with HOTf.[30] The ^{1}H NMR spectrum of the yellow crystalline product **15** indicated the presence of $NHMe_2$, which we anticipated to be coordinated to the stibenium center. Prolonged exposure of solid samples of **15** to vacuum at room temperature did not remove the $NHMe_2$ ligand. In contrast to our NMR observations for **9e** and **14**, the ^{i}Pr substituents of **15** gave only a single resonance for the methyl groups in both the ^{1}H and ^{13}C NMR spectra of this compound, suggesting either a symmetrical or a fluxional structure for this compound.

The identity of **15** was further confirmed by X-ray crystallography (Figure 4).[31] The structural changes that are observed with the formation of the dimethylamine-stabilized stibenium

(29) Burck, S.; Gudat, D.; Nieger, M.; Du Mont, W.-W. *J. Am. Chem. Soc.* **2006**, *128*, 3946.

(30) An example of this approach employed for generation of a phosphenium cation can be found in: Dahl, O. *Tetrahedron Lett.* **1982**, *23*, 1493.

(31) For simplicity, discussion has been limited to only one of the two independent units of **15** in the unit cell. There are no significant differences in the bond lengths and angles between these two species.

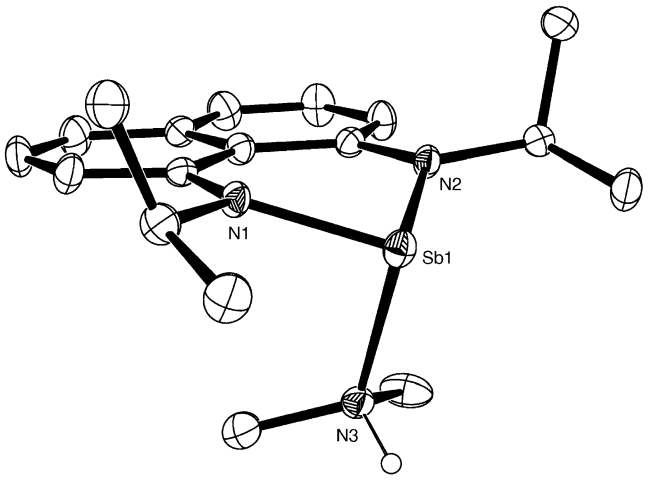

Figure 4. Thermal ellipsoid plot showing the molecular structure and partial atom numbering scheme of [Sb(^{i}PrN)$_2$C$_{10}$H$_6$·NHMe$_2$]-OTf (**15**) (only one of the two independent cations in the unit cell is shown). H atoms and triflate anion have been omitted for clarity.

cation **15** from **14** parallel those observed in the formation of **10a**−**d** and support our protonation approach to stibenium cation generation. Specifically, protonation of the dimethylamido nitrogen leads to a substantial increase in the Sb−N(3) bond length to 2.323(4) Å. Concomitant with this is a slight decrease in the Sb−N (napthalene) bond lengths (Sb−N(1) = 1.997(4) Å; Sb−N(2) = 2.000(4) Å) to values that are directly comparable to the those in the two previously reported examples of N-heterocyclic stibenium cations: [H$_2$C$_2$(N^{t}Bu)$_2$Sb] SbCl$_4$ (**2Sb**, R = ^{t}Bu, av. Sb−N = 2.024(2) Å)[11b] and [Me$_2$Si(N^{t}Bu)$_2$Sb]-AlCl$_4$ (**3Sb**, R = ^{t}Bu, av. Sb−N = 2.00(2) Å).[12] The Sb−N(3) bond length in **15** is significantly shorter than that observed in the NHMe$_2$ adduct of the neutral diamidochlorostibine [SbCl-(μ-N^{t}Bu)]$_2$ (Sb−N = 2.524(3) Å),[32] supporting the existence of a more electron-deficient cationic Sb center in [Sb-(^{i}PrN)$_2$C$_{10}$H$_6$·NHMe$_2$]OSO$_2$CF$_3$.

Consistent with the NMR observations, and as anticipated, the Sb(^{i}PrN)$_2$C$_{10}$H$_6$ framework adopted a more planar geometry as compared to **9e** or **14**. As well, the N(1)−Sb−N(2) angle observed in **15** (93.0(2)°) has increased by several degrees from that observed in the trisamidostibine **14** (86.2(2)°) and **9e** (86.5(2)°). This observation parallels the change in the N−Pn−N (Pn = P, As) angle that was observed with the conversion of diamidochloropnictines to the pnictogenium cations. It should be noted that the base-stabilized stibenium cation in **15** is well-separated from the triflate anion, the closest Sb−O contact being 2.823(9) Å in length.

Computational Studies. The results of density functional theory calculations on the pnictogenium components of **10a**−**d**, [E(RN)$_2$C$_{10}$H$_6$]$^+$ (E = P or As, R = ^{i}Pr or Ph) indicate that the nitrogen lone pairs are delocalized into the pnictogen p$_z$-orbital, forming strong π-bonding interactions in the heterocyclic ring. For the two isopropyl-based species, **10a**,**c**, the P/As lone pair of electrons is localized on the group 15 center and resides in a low-energy (HOMO − 4) orbital that is composed of substantial s-character and is oriented in the molecular plane and points away from the ring (Figure 5). An analogous bonding situation was revealed for the compounds **10b**,**d** with phenyl substitutents. In these two cations, the in-plane lone pairs were found to reside in a slightly lower HOMO − 9 level.[33]

(32) Edwards, A. J.; Leadbeater, N. E.; Paver, M. A.; Raithby, P. R.; Russell, C. A.; Wright, D. S. *J. Chem. Soc., Dalton Trans.* **1994**, 1479.

Both N-heterocyclic phosphenium and arsenium cations display interesting cation−cation interactions in the solid state, which appear to be primarily dependent on the identity of the nitrogen substituents rather than the identity of the group 15 element. As illustrated in Figure 6, the extended structures of the *N*-isopropyl substituted phosphenium and arsenium cations consist of dimers of π-stacked, antiparallel oriented cations. In the case of **10a**, the phosphenium center and gallate counterion are well-separated, whereas in the As analogue, **10c**, the pnictogenium center displays two long contacts between the arsenium center and two chlorine atoms located on a single tetrachlorogallate anion. The π-stacking, cation−cation contacts in the arsenium dimer are 3.35(1) Å in length (indicated in yellow in Figure 6b), whereas those in the phosphenium system are somewhat longer (3.47(1) Å). Cation−cation interactions between pnictogenium cations (**16**) have previously been observed by Burford and co-workers in dimers of the five-membered arsenium cation **4** (R = Me, Pn = As);[7] however, this dimerization occurs through As−N σ-bonds rather than through π-interactions. Interestingly, the related six-membered arsenium cations **5** (R = Me, Pn = As) do not form similar dimers.[8]

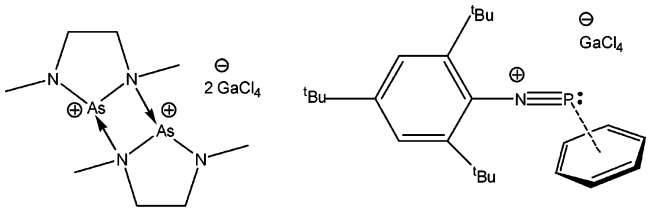

16 **17**

The *N*-phenyl substituted phosphenium and arsenium cations, **10b**,**d**, exhibit a different form of cation−cation interaction in the solid state, forming an extended network of zigzag chains as shown in Figure 7. In these head-to-tail chains, the cations are oriented in a perpendicular fashion with the pnictogenium center in one cation directed toward the centroid of a naphthalene ring on an adjacent cation. In the structure of **10b** (Figure 7a), the P-centroid distance of 3.426(7) Å is just beyond the sum of the van der Waals radii for phosphorus and carbon. As was the case with the *N*-isopropyl substituted cations, the arsenium cations of **10d** approach each other more closely with an As−centroid separation of 3.228(6) Å. Similar π-interactions with low-coordinate phosphorus centers are rare but not unprecedented in the literature; the phosphadiazonium cation, **17**, forms π-complexes with several arene solvents, where the length of the P−arene contact is dependent on the π-donor ability of the arene.[34] These interactions are analogous to those reported between tricoordinate As(III) centers and arenes.[35]

To examine the energetics of the interactions between the phosphenium cations in the stacked dimers of **10a**, full geometry optimizations were performed at the MP2/3-21G(d) level. These calculations revealed that the cation dimer exists in a minimum with a nominal separation between naphthalene rings of 3.25 Å (cf. 3.47(1) Å exptl). A detailed potential energy curve was

(33) Figures of the LUMO and pnictogenium lone pair orbitals for **10a**, **10b**, and **10d** are provided in the Supporting Information.

(34) (a) Burford, N.; Clyburne, J. A. C.; Bakshi, P. K.; Cameron, T. S. *Organometallics* **1995**, *14*, 1578. (b) Burford, N.; Clyburne, J. A. C.; Bakshi, P. K.; Cameron, T. S. *J. Am. Chem. Soc.* **1993**, *115*, 8829.

(35) (a) Schmidbaur, H.; Bublak, W.; Huber, B.; Müller, G. *Angew. Chem., Int. Ed. Engl.* **1987**, *26*, 234. (b) Probst, T.; Steigelmann, O.; Riede, H.; Schmidbaur, H. *Chem. Ber.* **1991**, *124*, 1089. (c) Schmidbaur, H.; Nowak, R.; Steigelmann, O.; Müller, G. *Chem. Ber.* **1990**, *123*, 1221.

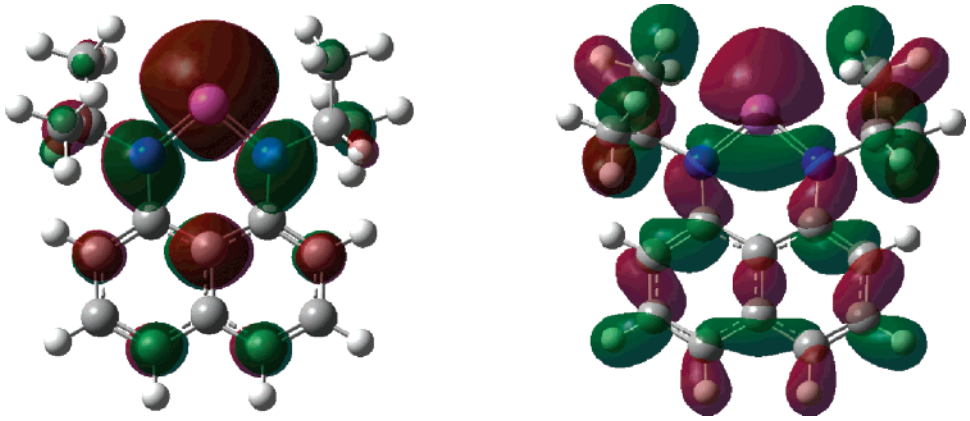

Figure 5. Orbital contour plots of As(^{i}PrN)$_2$C$_{10}$H$_6$]GaCl$_4$ (**10c**) showing the LUMO (left) and As-centered lone pair HOMO-4 (right) obtained from DFT calculations. Colors in these representations indicate the relative orbital phases. Compounds **10a**,**b**,**d** displayed analogous orbitals with similar configurations.[33]

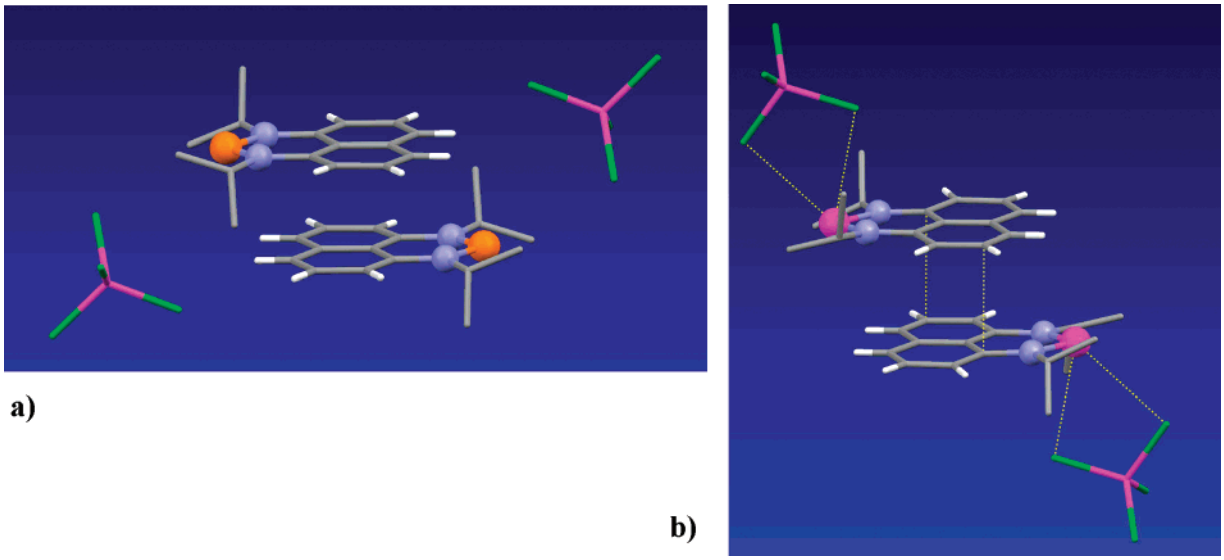

Figure 6. Representations of the π-stacked cation−cation interactions (dimers) that form in extended structures of (a) P(^{i}PrN)$_2$C$_{10}$H$_6$]-GaCl$_4$ (**10a**) and (b) As(^{i}PrN)$_2$C$_{10}$H$_6$]GaCl$_4$ (**10c**). H atoms on the isopropyl groups have been eliminated for clarity. Short contacts (less than sum of van der Waals radii) are shown in yellow.

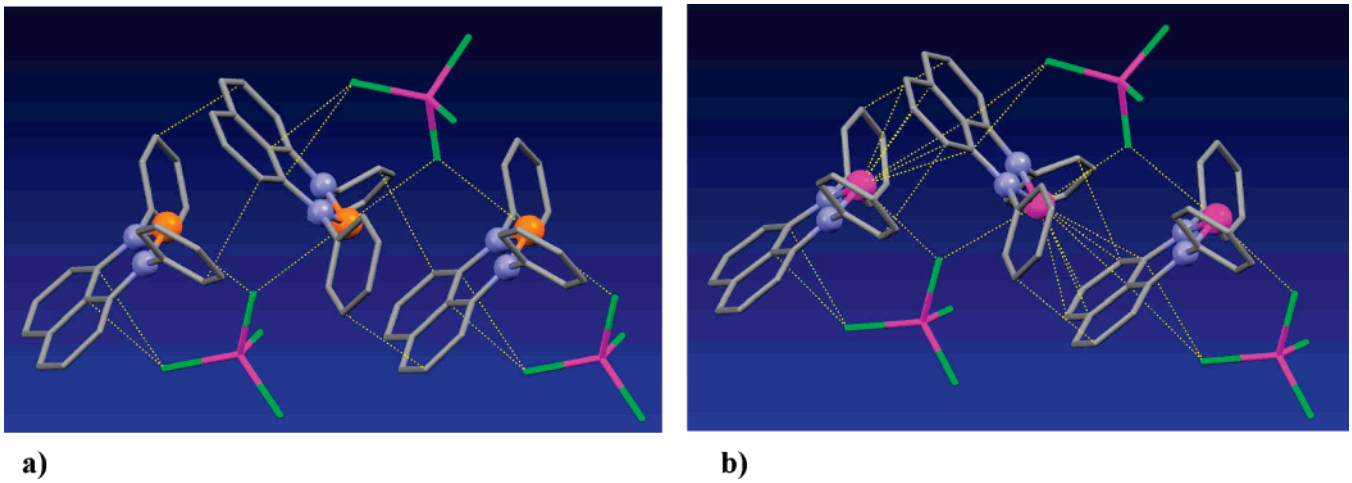

Figure 7. Representations of a portion of the extended, head-to-tail cation chains observed for (a) [P(PhN)$_2$C$_{10}$H$_6$]GaCl$_4$ (**10b**) and (b) [As(PhN)$_2$C$_{10}$H$_6$]GaCl$_4$ (**10d**). H atoms have been omitted for clarity. Short contacts (less than sum of van der Waals radii) are shown in yellow.

also calculated at the MP2/6-31G(d) level by incrementing the separation between rigid cation monomers along a vector perpendicular to the naphthalene rings (see Figure 6a). The calculated energies obtained from the scan are plotted in Figure 8. These calculations revealed that the stacked cation dimer of complex **10a** exists in a metastable minimum 22.5 kcal/mol

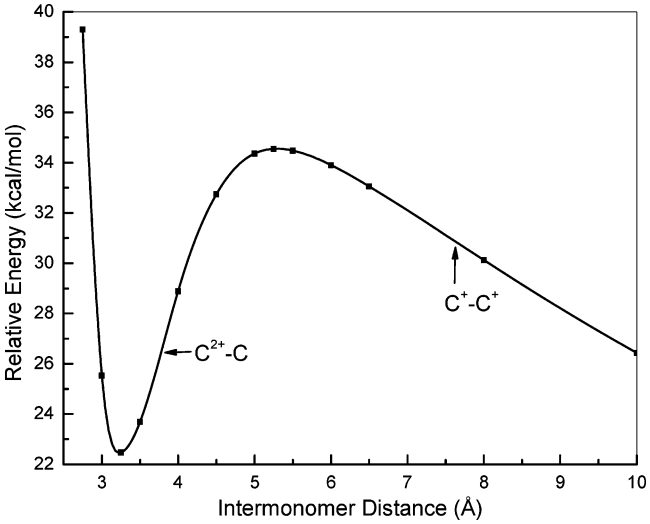

Figure 8. Potential energy curve showing the dissociation of phosphenium cation dimer in **10a** along the vector perpendicular to the naphthalene rings. Energies are relative to twice the monomer energy.

higher in energy relative to the separated cation monomers. The barrier to dissociation is 12.1 kcal/mol and occurs at a maximum separation of 5.25 Å. Additional calculations at selected points along the potential curve using MP2/6-311G(d) verified the smaller basis set results. The stacked cations are bound by dipole−dipole and dispersion interactions, and the metastability in the dimer complex can be understood as arising from the contribution of charge transfer states to the wavefunction of the dimer. The repulsive Coulombic interactions of the cation dimer complex, C^+-C^+, which occur at large separations, are overcome by a highly attractive charge transfer $C^{2+}-C$ state at short separations. This combination of attractive and repulsive forces results in a minimum in the potential energy curve (Figure 8) and creates a metastable system.

To make a more direct comparison between the cation structures bearing isopropyl and phenyl substituents, an optimized arsenium cation bearing *N*-methyl groups, $[As(MeN)_2C_{10}H_6]^+$, was used as a starting point. The goal was to employ a single, small substituent in an effort to reduce the role of sterics in this analysis. This species was then placed in the relative positions observed in the crystal structures of **10b**,**d**.[36] Single-point energies were then calculated for the π-stacked structure observed for **10b** and for the head-to-tail, T-shaped structure of **10d** both with and without one $GaCl_4^-$ counterion. The results indicated that, in the absence of the tetrachlorogallate anion, the π-stacked structure is more stable than the T-shaped structure by approximately 10.3 kcal/mol. This suggests that in terms of cation−cation interactions, the charge transfer states that allow formation of the metastable π-stacked structure contribute more to the cation−cation binding than does the pnictogen interaction with the naphthalene π-orbitals. In contrast, when the tetrachlorogallate anion was present, the stabilities were reversed with the T-shaped structure approximately 11.4 kcal/mol more stable than the π-stacked dimer. In this case, the structures are stable with respect to dissociation as a result of the counterion simultaneously stabilizing two arsenium cations.

From this analysis, we conclude that the different cation−cation interactions observed in the crystal structures for the two substituents arise principally from the steric differences between the isopropyl groups in **10a**,**c** and the phenyl groups in **10b**,**d**. The phenyl substituents do not allow a close enough approach of the cations along the π-stacking direction, thus reducing the stability provided by charge transfer and resulting in the alternative T-shaped head-to-tail structure with Pn$\cdots\pi$ interactions that was observed.

Conclusion

In conclusion, the library of known N-heterocyclic phosphenium, arsenium, and stibenium cations has been expanded to include examples supported by *N*,*N*′-disubstituted-1,8-diamidonaphthalene (R_2DAN^{2-}) ligation. These differ from the previously reported cations **2**−**6** in that the dicoordinate pnictogen atom is included in a six-membered ring forming part of an extended π-conjugated framework. The N-heterocyclic phosphenium and arsenium cations are readily prepared via pnictogen−chlorine bond heterolysis from the corresponding diamidochloropnictines **9a**−**d**; however, this procedure could not be extended to the heavier pnictogen antimony. Circumventing the usual halide abstraction route, the base-stabilized stibenium cation **15** was generated using a novel synthetic route involving protonation of an amido substituent. This reaction should be generally applicable to the synthesis of other low-coordinate pnictogen compounds.

The novel topology and electronic framework of the phosphenium and arsenium cations **10a**−**d** results in interesting substitution-dependent cation−cation interactions in the solid state. The *N*-isopropyl substituted cations **10a**,**c** form dimers through naphthyl π-stacking, while the *N*-phenyl substituted cations **10b**,**d** form extended zigzag chains through pnictogen−naphthalene π-interactions. Computational studies indicate that the π-stacked conformation, bound by dipole−dipole and dispersion interactions, is actually more energetically favorable than the chain structure; however, the steric demand of the phenyl ligands in **10b**,**d** impedes dimer formation. The Lewis amphoterism exhibited by the pnictogenium cations make them interesting ligands for transition metal coordination chemistry, and investigations in this area are currently underway.

Acknowledgment. This work was supported by the NSERC. H.A.S. is the recipient of an NSERC Postdoctoral Fellowship. G.A.D. thanks the Centre of Excellence in Integrated Nanotools for access to computational resources.

Supporting Information Available: CIF files for **9a**−**c**, **9e**, **10a**−**d**, **11b**, **14**, and **15**. LUMO and pnictogenium lone pair orbitals for **10a**,**b**,**d**. Results of HOMO−LUMO transition calculations for π-stacked pnictogenium complexes. Thermal ellipsoid plots for **9b** and **11b**. NMR data for *N*,*N*′-diphenyl-1,8-diaminonaphthalene. This material is available free of charge via the Internet at http://pubs.acs.org.

OM7004436

(36) Cation model used for these calculations was positioned to give the best fit with the cation positions in the crystal structures. This fitting procedure placed the atoms of the model structures within 0.1 Å of the corresponding atoms in the crystal structure. The single-point energy calculations were performed using MP2/6-31+G(d).

(37) Sheldrick, G. M. *SHELXTL 6.12*; Bruker AXS: Madison, WI, 2001.